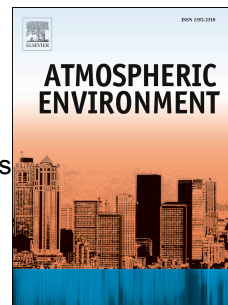


# Accepted Manuscript

Spatio-temporal variations and influencing factors of polycyclic aromatic hydrocarbons in atmospheric bulk deposition along a plain-mountain transect in western China

Xinli Xing, Yuan Zhang, Dan Yang, Jiaquan Zhang, Wei Chen, Chenxi Wu, Hongxia Liu, Shihua Qi



PII: S1352-2310(16)30368-5

DOI: [10.1016/j.atmosenv.2016.05.027](https://doi.org/10.1016/j.atmosenv.2016.05.027)

Reference: AEA 14615

To appear in: *Atmospheric Environment*

Received Date: 2 December 2015

Revised Date: 11 May 2016

Accepted Date: 14 May 2016

Please cite this article as: Xing, X., Zhang, Y., Yang, D., Zhang, J., Chen, W., Wu, C., Liu, H., Qi, S., Spatio-temporal variations and influencing factors of polycyclic aromatic hydrocarbons in atmospheric bulk deposition along a plain-mountain transect in western China, *Atmospheric Environment* (2016), doi: 10.1016/j.atmosenv.2016.05.027.

This is a PDF file of an unedited manuscript that has been accepted for publication. As a service to our customers we are providing this early version of the manuscript. The manuscript will undergo copyediting, typesetting, and review of the resulting proof before it is published in its final form. Please note that during the production process errors may be discovered which could affect the content, and all legal disclaimers that apply to the journal pertain.

1 **Spatio-temporal variations and influencing factors of Polycyclic**  
2 **Aromatic Hydrocarbons in atmospheric bulk deposition along a**  
3 **plain-mountain transect in Western China**

4  
5 Xinli Xing<sup>a,b</sup>, Yuan Zhang<sup>b</sup>, Dan Yang<sup>c</sup>, Jiaquan Zhang<sup>d,e</sup>, Wei Chen<sup>e</sup>, Chenxi Wu<sup>f</sup>, Hongxia Liu<sup>d</sup>, Shihua Qi<sup>a,b\*</sup>

6  
7 *a School of Environmental studies, China University of Geosciences, Wuhan, 430074, China*

8 *b State Key Laboratory of Biogeology and Environmental Geology, China University of Geosciences, Wuhan,*  
9 *430074, China*

10 *c Faculty of Engineering, China University of Geosciences, Wuhan 430074, China*

11 *d School of Environmental Science and Engineering, Hubei Polytechnic University, Huangshi 435003, China*

12 *e Lancaster Environmental Centre, Lancaster University, LA1 4YY, UK*

13 *f State Key Laboratory of Freshwater Ecology and Biotechnology, Institute of Hydrobiology, Chinese Academy of*  
14 *Sciences, Wuhan, 430072, China*

15  
16 **ABSTRACT**

17 Ten atmospheric bulk deposition (the sum of wet and dry deposition) samplers for polycyclic  
18 aromatic hydrocarbons (PAHs) were deployed at a plain-mountain transect (namely PMT transect,  
19 from Daying to Qingping) in Chengdu Plain, West China from June 2007 to June 2008 in four  
20 consecutive seasons (about every three months). The bulk deposition fluxes of  $\Sigma_{15}$ -PAHs ranged  
21 from 169.19  $\mu\text{g m}^{-2}\text{yr}^{-1}$  to 978.58  $\mu\text{g m}^{-2}\text{yr}^{-1}$  with geometric mean of 354.22  $\mu\text{g m}^{-2}\text{yr}^{-1}$ . The most  
22 prevalent PAHs were 4-ring (39.65%) and 3-ring (35.56%) PAHs. The flux values were  
23 comparable to those in rural areas. Higher fluxes of total PAHs were observed in the middle of  
24 PMT transect (SL, YX and JY, which were more urbanized than other sites). The seasonal  
25 deposition fluxes in the sampling profile indicated seasonality of the contaminant source was an  
26 important factor in controlling deposition fluxes. PAHs bulk deposition was negatively correlated  
27 with meteorological parameters (temperature, wind speed, humidity, and precipitation). No  
28 significant correlations between soil concentrations and atmospheric deposition were found along  
29 this transect. PAHs in soil samples had combined sources of coal, wood and petroleum combustion,  
30 while a simple source of coal, wood and grass combustion for bulk deposition. There were  
31 significant positive correlation relationship ( $p < 0.05$ ) between annual atmospheric bulk deposition  
32 and local PAHs emission, with biomass burning as the major contribution to the total emission of  
33 PAHs. This transect acts as an important PAHs source rather than being a sink according to the  
34 ratio of deposition/emission. Mountain cold trap effect existed in this transect where the altitude  
35 was higher than 1000 m. Long-range transport had an impact on the bulk deposition in summer.  
36 And this transect was a source to Tibetan only in summer. The forward trajectory analysis showed

---

\* Corresponding author. Tel.: +86 27 67883152, Fax: +86 27 87436235. E-mail addresses: [shihuaqi@cug.edu.cn](mailto:shihuaqi@cug.edu.cn) (Shihua Qi)

37 most air masses did not undergo long-range transport due to the blocking effect of surrounding  
38 mountains. Only a few air masses (<10%) arrived at the eastern and northern region of China or  
39 farther regions via long-range transport.

40

41 **Keywords:** Polycyclic aromatic hydrocarbons; Plain-mountain transect; Bulk deposition;  
42 Spatio-temporal variation; Influencing factor

43

#### 44 **1. Introduction**

45 Polycyclic aromatic hydrocarbons (PAHs) are ubiquitous environmental contaminants that  
46 are produced by anthropogenic emissions such as motor vehicles, industrial processes, domestic  
47 heating, waste incineration, tobacco smoke and by natural processes such as forest fires and  
48 volcanic eruptions (Keshtkar and Ashbaugh, 2007; Shen et al., 2013). PAHs are of great concern  
49 due to their widespread occurrence, long-range transport and toxic effects to ecosystem and  
50 human health (Wang et al., 2015).

51 Atmospheric deposition is the most important process that removes these chemicals from the  
52 atmosphere and are a major PAHs contributor in remote pristine areas(Wang et al., 2010).  
53 Atmospheric deposition is a potential important pathway of trace organic pollutants input to the  
54 land surface (Pan et al., 2013; Bari et al., 2014). In the wet deposition, PAHs are either dissolved  
55 in or rinsed by the rainfall or associated with particles. This process relies on the distribution of  
56 the organic matters diffused in vapor phase and particle phase, particle size distribution, and the  
57 Henry's law constant. Dry deposition of PAHs, on the other hand, is on accounted of association  
58 of PAHs with particles, related to the type of the surface, resistance to mass transfer in the  
59 deposition layer (Ollivon et al., 2002; Terzi and Samara, 2005). The total deposition consists of  
60 wet and dry deposition. However, it is hard to collect wet and dry deposition separately for  
61 long-term sampling especially in remote regions with insufficient electricity supply. Hence, the  
62 total deposition can be expressed by the sum of wet and dry deposition, namely "bulk" deposition,  
63 which does not discriminate any of the processes and , as a consequence, it sums up all of them  
64 (Motelay-Massei et al., 2003; Gocht et al., 2007; Esen et al., 2008; Zhang et al., 2008; Wang et al.,  
65 2011). Transport and fate of PAHs in the atmospheric bulk deposition partly depended on their  
66 physicochemical characteristics, atmospheric concentration, meteorological condition, topography  
67 and emission density (Gocht et al., 2007; Esen et al., 2008; Wang et al., 2011; Zhong and Zhu,  
68 2013). Conversely, the atmospheric deposition affected on the equilibrium partitioning of  
69 semi-volatile organic chemicals (SOCs) between air and surface, and finally had a strongly  
70 influence on the long-term distribution of SOCs in the regional/global environment. So the leading  
71 parameter in the process of SOCs transport varies from region to region (Schenker et al., 2014).

72 In western China, steep altitudinal transects separated the highly populated and intensively  
73 cultivated Chengdu Plain from the Tibetan Plateau. It is reported as important pathway of some  
74 persistent organic pollutants (POPs) from the vicinity of source regions in Chengdu Plain to the

75 Tibetan, which acts as the cold trap of airborne contaminants. Up to date, the majority of reports  
76 were focused on OCPs, PCBs, PCNs, PCDD/Fs and PBDEs in soil, atmosphere and biota in this  
77 region (Chen et al., 2008; Gong et al., 2010; Liu et al., 2010; Xing et al., 2010; Wang et al., 2012;  
78 Liu et al., 2013; Pan et al., 2013; Liu et al., 2014). However, information is limited on the  
79 atmospheric deposition contamination by PAHs in in this region. Sichuan Province is one of the  
80 most developed provinces in China and the total PAH emission in Sichuan ranked first in China  
81 in 2003 with average emission of  $5.35 \text{ kg km}^{-2}$  (Zhang et al., 2007). Hence, the impact of  
82 atmospheric deposition can not be ignored when studying the transport of PAHs and other  
83 similar contaminates.

84 This paper presents the result of atmospheric bulk deposition variation in the Chengdu  
85 Plain-mountain transect in western China with the aim of clarifying the role of Chengdu Plain as  
86 the primary emitter or middle path for POPs to Tibetan Plateau. Specifically, the main aims are:  
87 (1) clarifying the temporal and spatial characteristics of atmospheric deposition flux of PAHs; (2)  
88 to explore the key factor which affecting PAH deposition; and (3) to distinguish the potential role  
89 of this region (acting as a source or sink) according to the trajectory analysis.

## 90 **2. Experiment and methods**

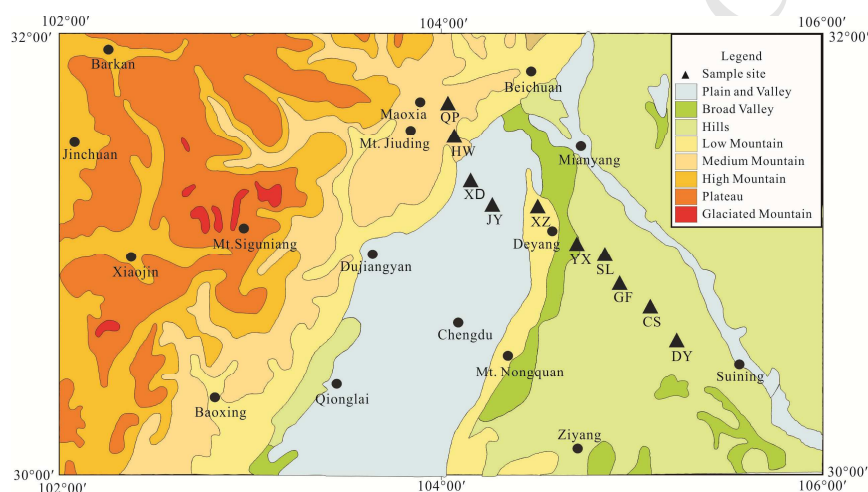
### 91 *2.1. Sampling*

92 The study region is located in the centre of Sichuan Province. The geography can be divided  
93 into four types: corrosive tectonic mountain of Tibetan Plateau east slope, Longmen Orogenic  
94 Piedmont Belt Accumulation Plain, Corrosive Tectonic Hills of east Sichuan Basin and Corrosive  
95 Tectonic Mountain of southwest Sichuan Basin. To describe PAHs deposition characteristic in this  
96 region, a typical plain-mountain transect was chosen, including low hills in the east, plain in the  
97 intergrades and high mountains in the west, which forms part of the eastern slope of Tibetan  
98 Plateau (Fig.1), namely "Plain-mountain transect (PMT)". The dominant wind direction (Southern  
99 east-northern west) in this region is also along this transect due to the presence of Tibetan in the  
100 northern west and monsoon climate in this region.

101 The atmospheric bulk deposition samplers were deployed at ten sites from Daying to  
102 Qingping during 16<sup>th</sup> June 2007 to 27<sup>th</sup> June 2008 (Fig.1). Detailed site information is listed in  
103 Table S1. The sampling programme was conducted for one year of four consecutive seasons  
104 (about every three months). The four periods from 16<sup>th</sup> June to 22<sup>nd</sup> September, 2007; 22<sup>nd</sup>  
105 September to 24<sup>th</sup> December, 2007; 24<sup>th</sup> December, 2007 to 22<sup>nd</sup> March 2008; and 22<sup>nd</sup> March  
106 2008 to 27<sup>th</sup> June 2008 were presented as summer, autumn, winter and spring respectively.

107 Bulk deposition (both dry and wet deposition) collection was achieved using a glass funnel  
108 with a receiving area of  $0.0225 \text{ m}^2$ , attached to a filter holder which was installed one meter above  
109 the ground or on the roof. Fallout was collected in a 4 L brown glass bottle wrapped with  
110 aluminium foil to prevent photodegradation. A long ring-shaped silica tube was used to link the  
111 funnel and collected bottle to conduct deposition and prevent volatilization. Prior to the field  
112 campaign, the funnels and the bottles were pre-cleaned using acid lotion and rinsed by deionized

113 water, then dried in an oven at 200 °C for 4 hours, and wrapped with aluminium foil. Before  
 114 set-up, each device was washed and triple rinsed with dichloromethane (DCM). Hydrated copper  
 115 sulphate ( $\text{CuSO}_4 \cdot 5\text{H}_2\text{O}$ ) was added to the bottles to inhibit microbial degradation. The tube was  
 116 washed with distilled water and DCM, and then wrapped with aluminium foil during transport to  
 117 the field (Fig.S1). Similar samplers were applied by many researchers (Ollivon et al., 2002;  
 118 Motelay-Massei et al., 2003; Gocht et al., 2007; Esen et al., 2008; Bari et al., 2014). When we  
 119 collected the bulk deposition, the surface soil samples were collected as well in the vicinity.  
 120 Totally, thirty-eight deposition samples and thirty-eight soil samples were collected. Bulk  
 121 deposition samples at two sites were destroyed during the Earthquake in May 2008. When  
 122 collecting, the funnels were cleaned with DCM three times and the washings were taken as a part  
 123 of bulk depositions. After collection, all the samples were preserved in ice boxes and transported  
 124 to the laboratory as soon as possible and stored at -20 °C before analysis.



125  
 126 Fig. 1 Sampling location for atmospheric deposition

## 127 2.2. Sample extraction and analysis

### 128 2.2.1. Extraction

129 The mixture of wet and dry atmospheric deposition samples were defrosted and homogenized  
 130 by shaking. Then the mixture was separated into the dissolved and particle parts by ultrafiltration  
 131 by shaking. Then the mixture was separated into the dissolved and particle parts by ultrafiltration  
 132 with a 0.45 $\mu\text{m}$  glass fibre filter membrane. The dissolved one was the water passed through filter  
 133 membrane and the particles were intercepted by the filter membrane. Both percolator and  
 134 membrane were cleaned three times by DCM before filtration. The membrane and particle  
 135 samples were wrapped with aluminium foil. Then particle and water were kept frozen at -20 °C  
 136 until analysis after about one week.

137 For the particle fraction, the same extraction procedure was followed as soil samples  
 138 extraction described previously (Xing et al., 2011). Generally, particle were injected with PAH  
 139 surrogates (naphthalene-d8, acenaphthene-d10, phenanthrene-d10, chrysene-d12 and  
 140 perylene-d12), and Soxhlet-extracted with dichloromethane (DCM) for 24 h. Small amount of  
 141 activated copper granules and anhydrous sodium sulphate were added to the extract, then the

142 extracts were concentrated and solvent-exchanged to hexane and further reduced to 1-2 mL by a  
143 rotary evaporator. A 1:2 (v/v) alumina/silica gel column was used to clean up the extract and  
144 targeted compounds were eluted with 30 ml of DCM/hexane (V:V=2:3). The eluate was then  
145 concentrated to 0.2 mL under a gentle pure nitrogen stream (purity  $\geq$  99.999%).  
146 Hexamethylbenzene was added as internal standard prior to instrumental analysis. The filtrated  
147 water was extracted using liquid-liquid extraction (LLE) method described in the literatures  
148 (Arias et al., 2009; Lohmann et al., 2009; Yang et al., 2013). Briefly, filtrated water was extracted  
149 with 40 mL of DCM and 2 g of anhydrous sodium sulphate in a separating funnel and shaken well  
150 for 4-5 minutes. The lower DCM layer was collected in a flat bottom flask and the remaining  
151 portion was extracted three times with 30 mL of DCM and the extracts were collected in a flat  
152 bottom flask. The extracts of water samples were then treated by the same method as particles  
153 extracts mentioned above. Finally, 0.2 mL eluate was obtained. Hexamethylbenzene was added as  
154 internal standard prior to instrumental analysis.

### 155 2.2.2. Analysis

156 Sixteen priority control PAHs recommended by the US Environmental Protection Agency  
157 were analysed using a GC-MS Agilent 6890N/5975MSD, equipped with a DB-5 capillary column  
158 (30 m  $\times$  0.25 mm diameter, 0.25  $\mu$ m film thickness) coupled in the electron impact mode (EI 70 eV,  
159 quadrupole temperature 150°C, ion source temperature 230°C). The chromatographic conditions  
160 were as follows: oven temperature program was initially at 60°C for 5 min and increased to 290°C  
161 at a rate of 3°C min<sup>-1</sup> and kept at 290°C for 40 min, while the temperature for injector and detector  
162 was maintained at 270°C and 280°C, respectively. The highly pure (99.999%) carrier gas was  
163 helium at a constant flow rate of 1.2 mL min<sup>-1</sup>. A 1  $\mu$ L concentrated sample was injected with  
164 splitless mode. The mass spectrometer was operated in the selected ion monitoring (SIM) mode  
165 and tuned with perfluorotributylamine (PFTBA) according to the manufacturer's specifications.  
166 Chromatographic peaks of samples were identified by mass spectra and retention time. The PAHs  
167 were quantitative analysed according to a 6-point calibration curve of reference materials with  
168 internal standard.

### 169 2.3. Quality control and quality assurance

170 Method blanks (solvent), spiked blanks (internal standard compounds spiked into solvent)  
171 and field blanks were analysed along with the sample batch. Moreover, 5  $\mu$ g mL<sup>-1</sup> PAHs standard  
172 solution were analysed by GC-MSD daily to estimate the method recovery as part of the  
173 instrumental quality control. Five PAHs surrogates consisting of naphthalene-D<sub>12</sub>,  
174 acenaphthene-D<sub>10</sub>, phenanthrene-D<sub>10</sub>, chrysene-D<sub>12</sub> and perylene-D<sub>12</sub> standards were spiked to  
175 each sample before extraction. The surrogate recoveries ranged from 70.1%-108.6%. The  
176 concentrations of PAHs were corrected by surrogate recoveries. The three times of the  
177 signal-to-noise level in the lowest concentration (0.2  $\mu$ g/mL) standard samples was used as the  
178 instrumental detection limit (IDLs). The IDLs of each substance was listed in Table S2. Mass  
179 spectrometry was evaluated by mass tuning. The retention times and areas of compounds in spiked

180 blanks were consistent with daily standard sample chromatograms. Calibration curves were was  
 181 adapted to period check with injection of standard solutions.

#### 182 2.4. Introductory remarks on the data set

183 Additional information on flux calculations, meteorological data sources, and a full list of  
 184 analytes is given in the supporting information Text S1.

### 185 3. Results and discussion

#### 186 3.1 General characteristic of annual deposition fluxes

187 Annual bulk deposition fluxes of PAHs were calculated and summary data are presented in  
 188 Table 1 and Fig S2. The results showed that total PAHs bulk deposition fluxes ranged from 169.19  
 189  $\mu\text{g m}^{-2}\text{yr}^{-1}$  at XZ to 978.58  $\mu\text{g m}^{-2}\text{yr}^{-1}$  at SL, with the geometric mean of 354.22  $\mu\text{g m}^{-2}\text{yr}^{-1}$ . The  
 190 proportion of PAH congeners along with the deposition profile was dominated by 3-ring (35.56%)  
 191 and 4-ring (39.65%) PAHs, followed by 5-6-ring (18.18%) and 2-ring (3.61%) PAHs, with the  
 192 fluxes of semivolatile PAHs Fla, Phe and Pry were higher than other PAHs on the annual basis.

193 The comparison of deposition fluxes in study area and other regions is listed in Tables S3.  
 194 The deposition flux in study area was comparable to those previously study in south China, it was  
 195 higher than that report in more industrialized or urbanized region like Pearl River Delta, China  
 196 during 2003-2004 ( $140\pm 89 \mu\text{g m}^{-2}\text{yr}^{-1}$ ) (Li et al., 2010), but it was slight lower than the report  
 197 value at Guangzhou during 2001-2002 (mean  $460 \mu\text{g m}^{-2}\text{yr}^{-1}$ ) (Li et al., 2009). The flux was much  
 198 less than the value in north China, where the deposition flux was  $5.22\pm 3.89 \mu\text{g m}^{-2}\text{day}^{-1}$  in  
 199 Beijing-Tianjin region (Wang et al., 2011),  $4.88\mu\text{g m}^{-2}\text{day}^{-1}$  in Tianjin and  $5.14 \mu\text{g m}^{-2}\text{day}^{-1}$  in the  
 200 rural of Beijing. Compared with other rural or suburban area in the world, the result was of same  
 201 order of magnitude as that reported in the rural of southern Germany ( $73.49\text{-}388.01\mu\text{g m}^{-2}\text{yr}^{-1}$ )  
 202 (Gocht et al., 2007), however it was higher than that in the suburban in the Seine Basin of France  
 203 ( $47.85\mu\text{g m}^{-2}\text{yr}^{-1}$ ) (Motelay-Massei et al., 2003), and that in remote site of northern Spain  
 204 ( $60.5\pm 16.4 \mu\text{g m}^{-2}\text{yr}^{-1}$ ) (Foan et al., 2015).

205 Table 1 Summary of annual bulk deposition ( $\mu\text{g m}^{-2}\text{yr}^{-1}$ ) of selected PAHs

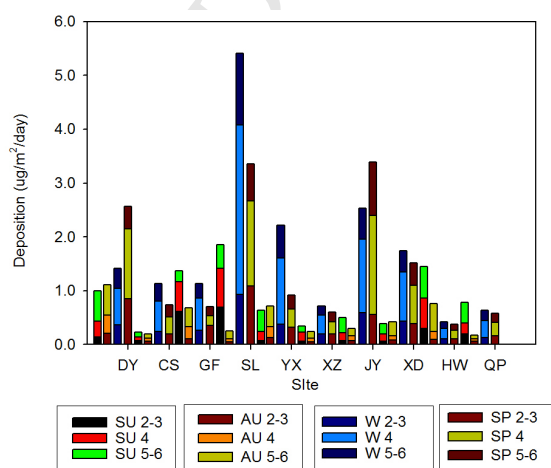
Compounds	Geometric mean	Average $\pm$ std	Median	Range
$\Sigma_{15}\text{PAHs}$	354.22	410.12 $\pm$ 248.56	358.87	169.19-978.58
Acy	1.45	3.58 $\pm$ 4.93	0.93	0.20 -14.37
Ace	0.22	0.25 $\pm$ 0.13	0.24	0.08-0.53
Flu	10.80	12.07 $\pm$ 5.82	11.76	4.57-23.42
Phe	61.88	71.55 $\pm$ 43.33	60.11	30.92-170.69
Ant	7.92	11.15 $\pm$ 11.87	6.47	3.60-41.78
Fla	63.35	78.44 $\pm$ 58.84	65.87	25.10-219.59
Pyr	43.33	53.24 $\pm$ 39.84	45.81	20.98-149.15
BaA	14.34	18.25 $\pm$ 14.43	12.73	6.17 -49.81-

Chr	30.18	35.48 ±21.43	29.32	15.49 -74.64-
BbF	29.36	32.34 ±13.67	32.46	12.09 -53.71
BkF	19.73	23.51±15.44	18.38	8.48 -58.29
BaP	12.28	13.42±5.87	13.89	6.28 -23.91
IcdP	24.02	27.22 ±13.76	23.90	9.86 -48.25
DahA	5.39	6.12 ±3.05	5.14	1.93 -10.77
BghiP	21.08	23.48 ±11.46	20.14	11.49 -42.19

206

207 *3.2 Spatial and seasonal variations of atmospheric deposition fluxes*

208 The geographic distribution of PAHs bulk deposition flux in four seasons is shown in Fig.2.  
 209 In general, higher fluxes of total PAHs were observed in the middle of this transect (DY, SL and  
 210 JY, the cities and towns around these sites are usually more industrialized or urbanized than in  
 211 remote sites); lower fluxes were observed at remote areas sites (HW and QP). The deposition  
 212 fluxes in SL were higher than in the surrounding rural areas sites and even higher than in JY, the  
 213 urban area site. The Shuanglong petrol station is on the opposite of SL site. Local point emission  
 214 in SL was an important reason for high deposition flux during sampling period possibly. Due to  
 215 the different physicochemical properties and sources of PAHs, there were spatial trends of  
 216 individual compounds. Higher proportion of 4-ring PAHs in higher deposition fluxes sites  
 217 indicated the 4-ring PAHs were the main contributor to the higher fluxes of bulk deposition.



218

219

Fig.2 The seasonal and spatial variation of different rings PAHs bulk deposition

220

(SU means summer samples, AU means autumn samples, W means winter samples and SP means spring samples.

221

And the numbers behind the capital letters mean the number of rings in the PAHs structure.)

222

223

For seasonal variation, the deposition fluxes in cold seasons (winter and spring) were higher  
 224 than those in warm seasons (summer and autumn). The high fluxes in winter and spring were  
 225 mainly due to a higher proportion of 4-ring PAHs than the other PAHs. 4-ring PAHs include Fla,  
 226 Pyr, BaA, and Chr. They are representative of coal combustion and vehicle emission source



227 (Khalili et al., 1995; Wang et al., 2008; Gregoris et al., 2014). In the cold seasons, more heating  
228 and warming demand will increase the combustion of coal, resulted in high emission of 4-ring  
229 PAHs. Meanwhile, the depositions of 4-ring PAHs in cold season were higher than in other  
230 seasons, indicating deposition of PAHs was consistent with the emission of PAHs. The seasonality  
231 of contaminant source could be an important factor in controlling the deposition fluxes. The result  
232 was in accordance with researches in other regions (Li et al., 2010; Wang et al., 2011). Besides the  
233 sources emission, the meteorological parameters are also decisive factors for the deposition fluxes.  
234 For example, temperature can affect the vapor-particle partitioning for SOCs (Jurado et al., 2004).  
235 And the intensity, form (rain or snow) and rate of precipitation, wind speed and humidity could  
236 have impacts on the washout ratio and/or dry deposition speed, which will cause the variation of  
237 deposition fluxes (Lei and Wania, 2004; Li et al., 2009). It means that the lower temperature and  
238 precipitation in the form of snow may have a higher scavenging ratio of PAHs in atmosphere.  
239 Moreover, the forest canopies can deplete of gaseous PAHs (Choi et al., 2008). Seasonal changes  
240 of forest canopies can affect the concentration of more volatile PAHs in the atmosphere. Thus the  
241 fluxes of PAHs with less rings in warm seasons was lower than those in the cold seasons.  
242 Comprehensively, all the above factors may result the seasonal varying of PAHs deposition fluxes.  
243 To clarify this issue in this junction between Chengdu Plain and east edge of Tibetan, the variation  
244 controlling factors of deposition fluxed are discussed below according to the collected data.

### 245 *3.3 Controlling factors for the atmospheric bulk deposition fluxes*

#### 246 *3.3.1 The influence of meteorological parameters on deposition fluxes*

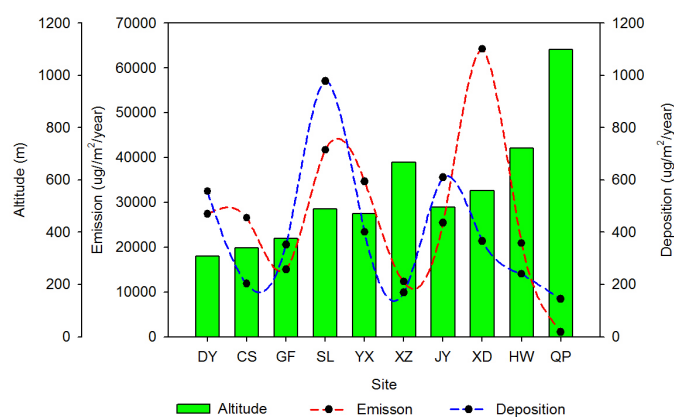
247 Meteorological conditions can affect PAHs in term of their generation, phase partition,  
248 diffusion, removal, etc.(He et al., 2014). The typical subtropical monsoon climate in Guangzhou  
249 played a key role in controlling seasonal variation of PAHs concentration and particle deposition  
250 fluxes (Li et al., 2010). High ambient temperature are correlated with low deposition rates in rural  
251 area of southern Germany (Gocht et al., 2007). The relationship between PAHs atmospheric bulk  
252 deposition and meteorological factors was analysed using IBM SPSS Statistics 20 and the  
253 Spearman correlation coefficients are shown in Table S4. Generally, negative relationship was  
254 found in mean of daily deposition bulk in every season versus temperature, wind speed, humidity,  
255 and precipitation for 4-rings and 2-3 rings PAH compounds. The deposition fluxes of 2-3 ring and  
256 4-ring PAHs were much higher than those of 5-6 ring PAHs (Fig.2). Hence, we can conclude  
257 PAHs bulk deposition was negatively correlated to those meteorological parameters. Similar  
258 results were reported in fine particulate matter in Nanjing, China (He et al., 2014) and particle  
259 deposition fluxes in Guangzhou (Li et al., 2010). However, for other POPs (e.g. pesticide such as  
260 HCHs and HCBs), stronger temperature dependencies were observed for high atmospheric  
261 concentration during warming periods and lower ones in the cold periods (Gioia et al., 2005). The  
262 possible reason was thermodynamically derived distribution (via evaporation from nearby  
263 terrestrial surfaces or long-range transport) for those compounds and primary emission density  
264 controlling patterns for PAHs in this study area.

265

## 266 3.3.2 The relationship between local emission and atmospheric deposition fluxes

267 As PAHs production is associated with anthropogenic activities such as domestic and  
 268 industrial heating, traffic petrol combustion, the population density as well, so the local emission  
 269 may explain the variations of PAHs deposition fluxes.

270 Local emission data was obtained from global atmospheric emission data of PAHs (Shen et  
 271 al., 2013) <http://inventory.pku.edu.cn/data/data.html>. The data we used was the annual average  
 272 value of the year 2007-2008 to match our sampling period. In the Fig.3, the total 15 PAHs bulk  
 273 deposition profile showed well coincides with the total local emission (2007-2008) in most  
 274 sampling site except for Site XD. As PAHs is associated with human activities, local emission can  
 275 be reflected on atmospheric bulk deposition fluxes. This transect is not only a pathway for PAHs  
 276 transport, but also an important source at low altitude region (except remote mountain site QP).



277

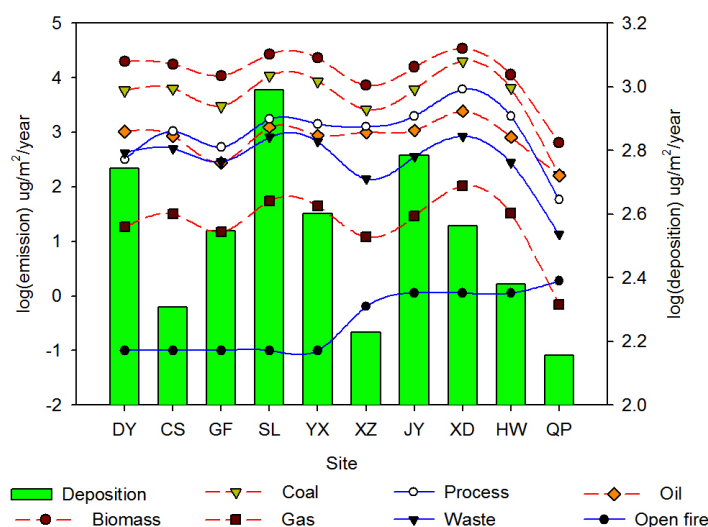
278

Fig.3  $\sum_{15}$ -PAHs bulk deposition vs. total local emission

279

280 In Fig. 4, the logarithm of the category of PAHs emission vs. bulk deposition was  
 281 demonstrated. The detailed information on every category was obtained from  
 282 <http://inventory.pku.edu.cn/data/data.html> (Shen et al., 2013), and the description of every  
 283 category can be found in the supporting information (Table S5). In Fig. 4, biomass combustion  
 284 presented the main contribution to the local emission of PAHs, secondly was coal, and then  
 285 followed by process, oil, waster, gas and open fire. There were obvious positive correlation  
 286 ( $p < 0.05$ ) between annual atmospheric bulk deposition and PAHs emission, especially with  
 287 biomass, oil and waste combustion (Table S6), which confirmed human activity affected the  
 288 deposition fluxes of PAHs. In addition, principal component analysis (PCA) was applied to  
 289 confirm the diagnostic testing. Total variability of the original data (depositions, biomass, coal, gas,  
 290 oil, process and waste) was represented during the PCA (Fig. S3). The first two principal  
 291 components (PCs), with eigenvalues greater than 1, accounted for 90.26% of the total variance in  
 292 the data set. As shown in Fig. S3, PC1, which explained 63.78% of the total variance, was highly  
 293 dominated by coal, gas, oil and process. It also had a large loading for biomass and waste. The  
 294 angles between deposition and the six emissions were all acute angles, indicating a positive

295 correlation between deposition and those emissions. PC2 accounted for 26.48% of the total  
 296 variance and was heavily weighted by deposition. PC2 had a high negative loading of open fire,  
 297 indicating no significant correlation of open fire with deposition.



298  
 299 Fig.4  $\Sigma_{15}$ -PAHs bulk deposition vs. different category emission in the form of logarithm

300 (For site DY, CS, GF, SL and YX, there was no open fire emission, for the transform of logarithm, -1 was given to  
 301 those values)

302  
 303 The emission fluxes of PAHs were hundreds of times higher than the deposition fluxes,  
 304 which indicated much more PAHs were preferentially transported to other area than to deposit in  
 305 local area, and thus this area was an important source region during the transport of PAHs. To  
 306 determine the role of this transect (source or sink), the relationship between deposition and  
 307 emission, the budget of deposition and emission were calculated. Firstly, the hypothesis deposition  
 308 from local emission totally was given. The deposition efficiency was calculated according to the  
 309 deposition divided by emission. In Fig.S4, the influence of altitude and molecular weight of PAHs  
 310 on the efficiency of deposition is shown. There was no obvious difference for site below 1000 m  
 311 a.s.l.. As the altitude increased more than 1000 m, the ratio of deposition/emission increased. One  
 312 possible reason was that the emission at region with higher altitude was less than that in Chengdu  
 313 Plain (Shen et al., 2013); another reason was mountain had a cold trap for POPs, especially for  
 314 heavy molecular weight compounds (Chen et al., 2008). 5-6 ring PAHs had higher  
 315 deposition/emission value than 2-3 and 4 ring PAHs. As rings of PAHs increased, the efficiency of  
 316 deposition was enhanced, which also suggested the light molecular PAHs had higher potentiality  
 317 to undergo long-range transport.

### 318 3.4 Effect of deposition on soil burdens

319 Soil plays an important role in the transport of POPs. It always acts as the sink during the  
 320 orographic cold trapping as altitude increases due to high precipitation rates and organic carbon  
 321 content (Daly and Wania, 2005; Daly et al., 2007; Chen et al., 2008; Choi et al., 2009; Sheng et al.,  
 322 2013), and simultaneously soil played the role of source for volatile compounds evaporation to  
 323 atmosphere when the equilibrium was broken between soil and air exchange (Cabrerizo et al.,

2011; Qu et al., 2015). The relationship between atmospheric deposition flux and soil concentration is shown in Fig.5. Generally, soil concentrations in most sites increased with altitude along this transect, and displayed maxima at intermediate elevations at XZ, a suburban site near Chengdu. These distribution patterns can be understood as being determined by the balance between atmospheric depositions and retention within the soils. However, for deposition flux, there was no significant increase. Neither significant correlations between soil concentrations and atmospheric deposition were observed along this transect. It also confirmed our conclusion that no thermodynamically distribution dominated in this region. The variation of PAHs concentration in soil was less than atmospheric deposition during different seasonal sampling, which possibly indicated soil was more stable than atmospheric deposition to the changes of PAHs emission, and thus explained why no positive relationship was found here for soil concentration and atmospheric deposition.

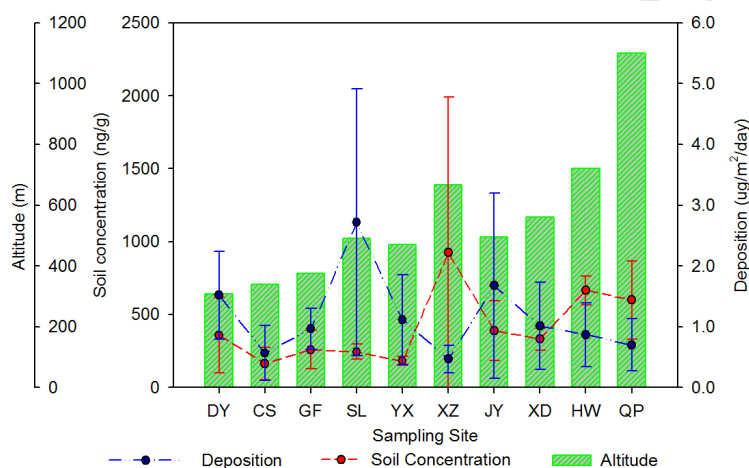


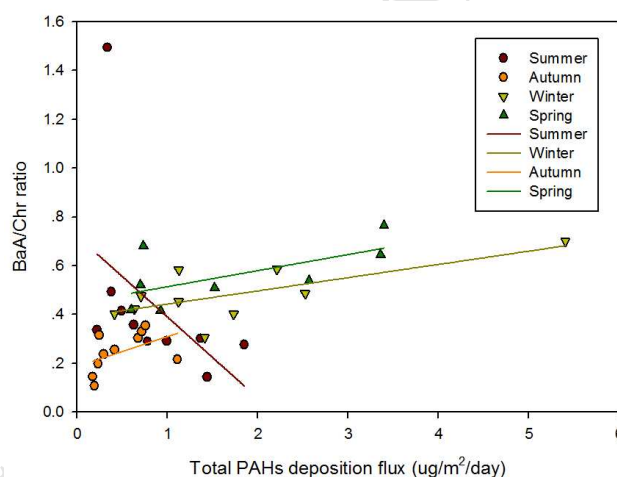
Fig. 5 Soil concentrations vs. atmospheric bulk deposition flux in sampling sites of different altitudes

The molecular indices IcdP/(IcdP + BghiP) and Flu/(Flu + Pyr) were used to distinguish the PAHs source for soil and atmospheric deposition in this study according to study in other regions (Ding et al., 2007; Xing et al., 2011; Gregoris et al., 2014; Bosch et al., 2015; Chen et al., 2015; Hong et al., 2015; Ma and Harrad, 2015; Zhang et al., 2015). The data for the ratios of these compounds in the atmospheric deposition and soil samples are presented in Fig.S5. The IcdP/(IcdP + BghiP) values for most samples were >0.5, suggesting that coal and wood combustion may be the predominant source of PAHs in atmospheric deposition, while PAHs ratios in soils were mainly between 0.3-0.7, indicating a more complicated PAHs sources derived from mixed combustion of coal wood and petroleum combustion. The ratios of Fla/(Fla + Pry) from atmospheric deposition showed PAHs mainly derived from combustion of coal, wood and grass as well. However, PAHs in soil arise from a complex mixture of sources, including both biomass combustion as well as fossil fuel combustion, which fits well with the result from IcdP/(IcdP + BghiP). According to biplots of IcdP/(IcdP + BghiP) versus Fla/(Fla + Pry) ratio for soil and atmospheric deposition, the results suggested combustion of coal, grass and wood was major

353 source of PAHs in atmospheric deposition, while soil arose from a complex mixture of sources,  
 354 including both combustion for rooms heating and cooking, as well as outdoor emissions from  
 355 traffic and fossil fuel combustion. This result confirmed why no positive relationship was shown  
 356 for soil and atmospheric deposition.

### 357 3.5 Influence of regional atmospheric transport of PAHs on deposition fluxes

358 Air mass transport can bring in pollutants from distance areas, thus affecting local PAHs  
 359 concentration in atmosphere. It was reported that the impact of local or regional transport can be  
 360 reflected by the ratio of more reactive PAHs to a stable PAH, such as the ratio of BaA/Chr can be  
 361 employed to illustrate whether the collected air masses are fresh or aged. A higher ratio indicates  
 362 relatively little photochemical processing of the air mass and major impact from local emissions.  
 363 On the other hand, a lower ratio is reflective of more aged PAHs (Ding et al., 2007). Fig. 6  
 364 revealed the relationship between BaA/Chr and PAHs deposition fluxes in different seasons.  
 365 Generally, a slight positive relationship was shown during the periods of autumn, winter and  
 366 spring, as PAHs deposition increased, the ratios of BaA/Chr become higher, indicating the  
 367 elevated deposition was mainly contribution of local emission. While in summer sampling periods,  
 368 a negative relationship was presented, illuminating long-range transport had a higher impact on  
 369 the deposition in summer.



370  
 371 Fig.6 The relationship between BaA/Chr and PAHs deposition fluxes

372

373 In order to identify potential source regions and transport pathways, 5-day backward and  
 374 forward trajectories arriving at 100 meters above ground level for one year between June 2007  
 375 and June 2008 at the sampling site were generated using the PC Version HYSPLIT 4 model  
 376 (<http://www.arl.noaa.gov/ready/hysplit4.html>) respectively. This model was developed by  
 377 NOAA/ARL (US National Oceanic and Atmospheric Administration/Air Resources Laboratory).  
 378 The seasonal trajectories after cluster are presented in Fig.S6 and Fig.S7.

379 The back trajectory maps are shown in Fig.S6, which indicated local emissions were the  
 380 dominant source (more than 40 % of total air mass) for PAHs deposition in the study area during  
 381 sampling time. Second source was the eastern and northern part of China. The air mass from the

382 countries west to China such as Indian and Nepal, which underwent long-rang transport also  
383 arrived in this region. In summer, during the summer monsoon period, a high percentage  
384 contribution (21% of air masses) from the south of China entered the study area as well. It  
385 confirmed our conclusion that the long-range transport has a higher impact on the atmospheric  
386 deposition during summer. The annual back trajectory map showed the same result as the seasonal  
387 conclusions. Most air masses were originated from local or nearby regions (36%). Due to the  
388 influence of eastern monsoon, the high contribution (28%) was from eastern region as well,  
389 followed by air mass from the north of China (23%). The air mass from west direction underwent  
390 long distance transport, and had small contribution (7% and 6%) to the total air mass in the study  
391 region. It indicated the spatial variation in bulk deposition was mainly effected by the local  
392 emission in our study. As mentioned above, only a little local emission PAHs was loaded in situ,  
393 most PAHs may undergo long-rang transport to other region. The study in Wolong near our study  
394 area reported air mass from lower altitude Chengdu might enter western mountains (Pan et al.,  
395 2013). The forward trajectory maps (Fig.S7) show the possible sink/fate of pollutants originated  
396 from our study area. In summer, about 10% of air masses originating from the Chengdu Plain  
397 indeed entered the western part of China, e.g. the Tibet. However, most air masses did not undergo  
398 long-range transport. The mountains surrounding Chengdu Plain blocked them. Only a small  
399 fraction of air masses (<10%) which underwent long-range transport, the main destinations were  
400 the eastern and northern regions of China or farther regions.

401

#### 402 4. Conclusions

403 The bulk deposition fluxes of  $\sum_{15}$ -PAHs ranged from  $169.19 \mu\text{g m}^{-2} \text{yr}^{-1}$  to  $978.58 \mu\text{g m}^{-2} \text{yr}^{-1}$ ,  
404 with the geometric mean of  $354.22 \mu\text{g m}^{-2} \text{yr}^{-1}$  along a plain–mountain transect in Chengdu Plain,  
405 West China, from Daying to Qingping. Higher fluxes of total PAHs were observed in the middle  
406 of this transect (urbanized sites, SL, YX and JY). The deposition fluxes of  $\sum_{15}$ -PAHs in cold  
407 seasons (winter and spring) were higher than those in warm seasons (summer and autumn),  
408 indicating that the seasonal variation of contaminant source was an important factor in controlling  
409 the deposition fluxes.

410 PAHs bulk deposition was negatively correlated with meteorological parameters (temperature,  
411 wind speed, humidity and precipitation). No significant correlations were found between soil  
412 concentrations and atmospheric deposition along this transect. The biplots of  $\text{IcdP}/(\text{IcdP} + \text{BghiP})$   
413 vs.  $\text{Fla}/(\text{Fla} + \text{Pry})$  indicated a more complex source for soil while simple combustion source of  
414 coal, wood and grass for bulk deposition was shown. There were obvious positive correlation  
415 ( $p < 0.05$ ) between annual atmospheric bulk deposition and PAHs emission, and biomass was the  
416 main contributor to the total emission of PAHs.

417 According to the ratio of deposition/emission, this transect played an important role as a  
418 source of PAHs rather than a sink. Mountain cold trap existed in this transect where altitude was

419 higher than 1000 meters. The ratio of BaA/Chr and back trajectory indicated that high atmospheric  
420 deposition was closely associated with local emission. While long-range transport had an  
421 important impact on the deposition fluxes in summer. The forward trajectory illuminated this  
422 transect was a source to Tibet only in summer. Most air mass in this study did not undergo  
423 long-range transport due to the blocking effect of surrounding mountains. Only a few air masses  
424 (<10%) underwent long-range transport to the eastern and northern regions of China or farther  
425 regions.

426

#### 427 **Acknowledgements**

428 This study was financially supported by the National Natural Science Foundation of China  
429 (No 41103065, 41473095, 41473095). Xinli Xing and Jiaquan Zhang gratefully acknowledge the  
430 financial support from China Scholarship Council. The authors are grateful to Feng Xu, Yuan Gao,  
431 Fang Tian for their help in the field sampling work. Thanks Professor Shu Tao from Peking  
432 University supporting us the local PAHs emission data.

433

#### 434 **References**

435 Arias, A.H., Spetter, C.V., Freije, R.H., Marcovecchio, J.E., 2009. Polycyclic aromatic hydrocarbons in  
436 water, mussels (*Brachidontes* sp., *Tagelus* sp.) and fish (*Odontesthes* sp.) from Bahía Blanca Estuary,  
437 Argentina. *Estuarine, Coastal and Shelf Science* 85, 67-81.

438 Bari, M.A., Kindzierski, W.B., Cho, S., 2014. A wintertime investigation of atmospheric deposition of  
439 metals and polycyclic aromatic hydrocarbons in the Athabasca Oil Sands Region, Canada. *Science of  
440 the Total Environment* 485, 180-192.

441 Bosch, C., Andersson, A., Krusa, M., Bandh, C., Hovorkova, I., Klanova, J., Knowles, T.D.J., Pancost,  
442 R.D., Evershed, R.P., Gustafsson, O., 2015. Source Apportionment of Polycyclic Aromatic  
443 Hydrocarbons in Central European Soils with Compound-Specific Triple Isotopes ( $\delta^{13}\text{C}$ ,  $\delta^2\text{H}$ , and  $\delta^3\text{S}$ ). *Environmental Science & Technology* 49, 7657-7665.

445 Cabrerizo, A., Dachs, J., Jones, K.C., Barcelo, D., 2011. Soil-Air exchange controls on background  
446 atmospheric concentrations of organochlorine pesticides. *Atmospheric Chemistry and Physics* 11,  
447 12799-12811.

448 Chen, D., Liu, W., Liu, X., Westgate, J.N., Wania, F., 2008. Cold-trapping of persistent organic  
449 pollutants in the mountain soils of Western Sichuan, China. *Environmental Science & Technology* 42,  
450 9086-9091.

451 Chen, P.F., Kang, S.C., Li, C.L., Rupakheti, M., Yan, F.P., Li, Q.L., Ji, Z.M., Zhang, Q.G., Luo, W.,  
452 Sillanpaa, M., 2015. Characteristics and sources of polycyclic aromatic hydrocarbons in atmospheric  
453 aerosols in the Kathmandu Valley, Nepal. *Science of the Total Environment* 538, 86-92.

454 Choi, S.-D., Shunthirasingham, C., Daly, G.L., Xiao, H., Lei, Y.D., Wania, F., 2009. Levels of  
455 polycyclic aromatic hydrocarbons in Canadian mountain air and soil are controlled by proximity to  
456 roads. *Environmental Pollution* 157, 3199-3206.

457 Choi, S.D., Staebler, R.M., Li, H., Su, Y., Gevaio, B., Harner, T., Wania, F., 2008. Depletion of gaseous

- 458 polycyclic aromatic hydrocarbons by a forest canopy. *Atmospheric Chemistry and Physics* 8,  
459 4105-4113.
- 460 Daly, G.L., Lei, Y.D., Teixeira, C., Muir, D.C.G., Wania, F., 2007. Pesticides in western Canadian  
461 mountain air and soil. *Environmental Science & Technology* 41, 6020-6025.
- 462 Daly, G.L., Wania, F., 2005. Organic contaminants in mountains. *Environmental Science & Technology*  
463 39, 385-398.
- 464 Ding, X., Wang, X.-M., Xie, Z.-Q., Xiang, C.-H., Mai, B.-X., Sun, L.-G., Zheng, M., Sheng, G.-Y., Fu,  
465 J.-M., Pöschl, U., 2007. Atmospheric polycyclic aromatic hydrocarbons observed over the North  
466 Pacific Ocean and the Arctic area: Spatial distribution and source identification. *Atmospheric*  
467 *Environment* 41, 2061-2072.
- 468 Esen, F., Cindoruk, S.S., Tasdemir, Y., 2008. Bulk deposition of polycyclic aromatic hydrocarbons  
469 (PAHs) in an industrial site of Turkey. *Environmental Pollution* 152, 461-467.
- 470 Foan, L., Domercq, M., Bermejo, R., Miguel Santamaria, J., Simon, V., 2015. Mosses as an integrating  
471 tool for monitoring PAH atmospheric deposition: Comparison with total deposition and evaluation of  
472 bioconcentration factors. A year-long case-study. *Chemosphere* 119, 452-458.
- 473 Gioia, R., Offenberg, J.H., Gigliotti, C.L., Totten, L.A., Du, S., Eisenreich, S.J., 2005. Atmospheric  
474 concentrations and deposition of organochlorine pesticides in the US Mid-Atlantic region. *Atmospheric*  
475 *Environment* 39, 2309-2322.
- 476 Gocht, T., Klemm, O., Grathwohl, P., 2007. Long-term atmospheric bulk deposition of polycyclic  
477 aromatic hydrocarbons (PAHs) in rural areas of Southern Germany. *Atmospheric Environment* 41,  
478 1315-1327.
- 479 Gong, P., Wang, X., Sheng, J., Yao, T., 2010. Variations of organochlorine pesticides and  
480 polychlorinated biphenyls in atmosphere of the Tibetan Plateau: Role of the monsoon system.  
481 *Atmospheric Environment* 44, 2518-2523.
- 482 Gregoris, E., Argiriadis, E., Vecchiato, M., Zambon, S., De Pieri, S., Donato, A., Contini, D., Piazza,  
483 R., Barbante, C., Gambaro, A., 2014. Gas-particle distributions, sources and health effects of polycyclic  
484 aromatic hydrocarbons (PAHs), polychlorinated biphenyls (PCBs) and polychlorinated naphthalenes  
485 (PCNs) in Venice aerosols. *Science of the Total Environment* 476-477, 393-405.
- 486 He, J., Fan, S., Meng, Q., Sun, Y., Zhang, J., Zu, F., 2014. Polycyclic aromatic hydrocarbons (PAHs)  
487 associated with fine particulate matters in Nanjing, China: Distributions, sources and meteorological  
488 influences. *Atmospheric Environment* 89, 207-215.
- 489 Hong, Y.W., Chen, J.S., Zhang, F.W., Zhang, H., Xu, L.L., Yin, L.Q., Chen, Y.T., 2015. Effects of  
490 urbanization on gaseous and particulate polycyclic aromatic hydrocarbons and polychlorinated  
491 biphenyls in a coastal city, China: levels, sources, and health risks. *Environmental Science and*  
492 *Pollution Research* 22, 14919-14931.
- 493 Jurado, E., Jaward, F.M., Lohmann, R., Jones, K.C., Simo, R., Dachs, J., 2004. Atmospheric dry  
494 deposition of persistent organic pollutants to the Atlantic and inferences for the global oceans.  
495 *Environmental Science & Technology* 38, 5505-5513.
- 496 Keshtkar, H., Ashbaugh, L.L., 2007. Size distribution of polycyclic aromatic hydrocarbon particulate  
497 emission factors from agricultural burning. *Atmospheric Environment* 41, 2729-2739.



- 498 Lei, Y.D., Wania, F., 2004. Is rain or snow a more efficient scavenger of organic chemicals?  
499 Atmospheric Environment 38, 3557-3571.
- 500 Li, J., Cheng, H., Zhang, G., Qi, S., Li, X., 2009. Polycyclic aromatic hydrocarbon (PAH) deposition to  
501 and exchange at the air-water interface of Luhu, an urban lake in Guangzhou, China. Environmental  
502 Pollution 157, 273-279.
- 503 Li, J., Liu, X., Zhang, G., Li, X.-D., 2010. Particle deposition fluxes of BDE-209, PAHs, DDTs and  
504 chlordanes in the Pearl River Delta, South China. Science of the Total Environment 408, 3664-3670.
- 505 Liu, H., Qi, S., Yang, D., Hu, Y., Li, F., Liu, J., Xing, X., 2013. Soil concentrations and soil-air  
506 exchange of organochlorine pesticides along the Abo profile, east of the Tibetan Plateau, western China.  
507 Frontiers of Earth Science 7, 395-405.
- 508 Liu, W., Chen, D., Liu, X., Zheng, X., Yang, W., Westgate, J.N., Wania, F., 2010. Transport of  
509 semivolatile organic compounds to the Tibetan Plateau: spatial and temporal variation in air  
510 concentrations in mountainous Western Sichuan, China. Environmental Science & Technology 44,  
511 1559-1565.
- 512 Liu, X., Li, J., Zheng, Q., Bing, H., Zhang, R., Wang, Y., Luo, C., Liu, X., Wu, Y., Pan, S., Zhang, G.,  
513 2014. Forest Filter Effect versus Cold Trapping Effect on the Altitudinal Distribution of PCBs: A Case  
514 Study of Mt. Gongga, Eastern Tibetan Plateau. Environmental Science & Technology 48, 14377-14385.
- 515 Lohmann, R., Gioia, R., Jones, K.C., Nizzetto, L., Temme, C., Xie, Z., Schulz-Bull, D., Hand, I.,  
516 Morgan, E., Jantunen, L., 2009. Organochlorine pesticides and PAHs in the surface water and  
517 atmosphere of the North Atlantic and Arctic Ocean. Environmental Science & Technology 43,  
518 5633-5639.
- 519 Ma, Y.N., Harrad, S., 2015. Spatiotemporal analysis and human exposure assessment on polycyclic  
520 aromatic hydrocarbons in indoor air, settled house dust, and diet: A review. Environment International  
521 84, 7-16.
- 522 Motelay-Massei, A., Ollivon, D., Garban, B., Chevreuril, M., 2003. Polycyclic aromatic hydrocarbons  
523 in bulk deposition at a suburban site: assessment by principal component analysis of the influence of  
524 meteorological parameters. Atmospheric Environment 37, 3135-3146.
- 525 Ollivon, D., Blanchoud, H., Motelay-Massei, A., Garban, B., 2002. Atmospheric deposition of PAHs to  
526 an urban site, Paris, France. Atmospheric Environment 36, 2891-2900.
- 527 Pan, J., Yang, Y., Zhu, X., Yeung, L.W.Y., Taniyasu, S., Miyake, Y., Falandysz, J., Yamashita, N., 2013.  
528 Altitudinal distributions of PCDD/Fs, dioxin-like PCBs and PCNs in soil and yak samples from  
529 Wolong high mountain area, eastern Tibet-Qinghai Plateau, China. Science of the Total Environment  
530 444, 102-109.
- 531 Qu, C., Qi, S., Yang, D., Huang, H., Zhang, J., Chen, W., Yohannes, H.K., Sandy, E.H., Yang, J., Xing,  
532 X., 2015. Risk assessment and influence factors of organochlorine pesticides (OCPs) in agricultural  
533 soils of the hill region: A case study from Ningde, southeast China. Journal of Geochemical  
534 Exploration 149, 43-51.
- 535 Schenker, S., Scheringer, M., Hungerbühler, K., 2014. Do persistent organic pollutants reach a  
536 thermodynamic equilibrium in the global environment? Environmental Science & Technology 48,  
537 5017-5024.

- 538 Shen, H.Z., Huang, Y., Wang, R., Zhu, D., Li, W., Shen, G.F., Wang, B., Zhang, Y.Y., Chen, Y.C., Lu, Y.,  
539 Chen, H., Li, T.C., Sun, K., Li, B.G., Liu, W.X., Liu, J.F., Tao, S., 2013. Global Atmospheric Emissions  
540 of Polycyclic Aromatic Hydrocarbons from 1960 to 2008 and Future Predictions. *Environmental*  
541 *Science & Technology* 47, 6415-6424.
- 542 Sheng, J.J., Wang, X.P., Gong, P., Joswiak, D.R., Tian, L.D., Yao, T.D., Jones, K.C., 2013.  
543 Monsoon-Driven Transport of Organochlorine Pesticides and Polychlorinated Biphenyls to the Tibetan  
544 Plateau: Three Year Atmospheric Monitoring Study. *Environmental Science & Technology* 47,  
545 3199-3208.
- 546 Terzi, E., Samara, C., 2005. Dry deposition of polycyclic aromatic hydrocarbons in urban and rural  
547 sites of Western Greece. *Atmospheric Environment* 39, 6261-6270.
- 548 Wang, C.h., Wu, S.h., Zhou, S.l., Wang, H., Li, B.j., Chen, H., Yu, Y.n., Shi, Y.x., 2015. Polycyclic  
549 aromatic hydrocarbons in soils from urban to rural areas in Nanjing: Concentration, source, spatial  
550 distribution, and potential human health risk. *Science of the Total Environment* 527, 375-383.
- 551 Wang, R., Tao, S., Wang, B., Yang, Y., Lang, C., Zhang, Y., Hu, J., Ma, J., Hung, H., 2010. Sources and  
552 Pathways of Polycyclic Aromatic Hydrocarbons Transported to Alert, the Canadian High Arctic.  
553 *Environmental Science & Technology* 44, 1017-1022.
- 554 Wang, W., Simonich, S.L.M., Giri, B., Xue, M., Zhao, J., Chen, S., Shen, H., Shen, G., Wang, R., Cao,  
555 J., Tao, S., 2011. Spatial distribution and seasonal variation of atmospheric bulk deposition of  
556 polycyclic aromatic hydrocarbons in Beijing-Tianjin region, North China. *Environmental Pollution* 159,  
557 287-293.
- 558 Wang, X.-p., Sheng, J.-j., Gong, P., Xue, Y.-g., Yao, T.-d., Jones, K.C., 2012. Persistent organic  
559 pollutants in the Tibetan surface soil: Spatial distribution, air-soil exchange and implications for global  
560 cycling. *Environmental Pollution* 170, 145-151.
- 561 Xing, X.L., Qi, S.H., Zhang, J.Q., Wu, C.X., Zhang, Y., Yang, D., Odhiambo, J.O., 2011. Spatial  
562 distribution and source diagnosis of polycyclic aromatic hydrocarbons in soils from Chengdu  
563 Economic Region, Sichuan Province, western China. *Journal of Geochemical Exploration* 110,  
564 146-154.
- 565 Xing, X.L., Qi, S.H., Zhang, Y.A., Yang, D., Odhiambo, J.O., 2010. Organochlorine Pesticides (OCPs)  
566 in Soils Along the Eastern Slope of the Tibetan Plateau. *Pedosphere* 20, 607-615.
- 567 Yang, D., Qi, S., Zhang, Y., Xing, X., Liu, H., Qu, C., Liu, J., Li, F., 2013. Levels, sources and potential  
568 risks of polycyclic aromatic hydrocarbons (PAHs) in multimedia environment along the Jinjiang River  
569 mainstream to Quanzhou Bay, China. *Marine Pollution Bulletin* 76, 298-306.
- 570 Zhang, G., Chakraborty, P., Li, J., Sampathkumar, P., Balasubramanian, T., Kathiresan, K., Takahashi,  
571 S., Subramanian, A., Tanabe, S., Jones, K.C., 2008. Passive Atmospheric Sampling of Organochlorine  
572 Pesticides, Polychlorinated Biphenyls, and Polybrominated Diphenyl Ethers in Urban, Rural, and  
573 Wetland Sites along the Coastal Length of India. *Environmental Science & Technology* 42, 8218-8223.
- 574 Zhang, Y., Yu, H.J., Xi, B.D., Hou, H.B., Gao, R.T., Liang, Q., Zhang, H., Xu, F.X., 2015. Levels,  
575 sources, and potential ecological risks of polycyclic aromatic hydrocarbons (PAHs) in a typical  
576 effluent-receiving river (Wangyang River), North China. *Arabian Journal of Geosciences* 8, 6535-6543.
- 577 Zhang, Y.X., Tao, S., Cao, J., Coveney, R.M., 2007. Emission of polycyclic aromatic hydrocarbons in

- 578 China by county. Environmental Science & Technology 41, 683-687.
- 579 Zhong, Y., Zhu, L., 2013. Distribution, input pathway and soil-air exchange of polycyclic aromatic
- 580 hydrocarbons in Banshan Industry Park, China. Science of the Total Environment 444, 177-182.
- 581
- 582

ACCEPTED MANUSCRIPT

**Highlights:**

- Spatio-temporal variations of PAHs in atmospheric deposition were observed.
- PAHs deposition was negatively correlated to some meteorological parameters.
- Atmospheric PAHs deposition was closely related to local emission.
- This transect played an important role of source rather than sink.
- Most air mass did not undergo long-range transport due to the presence of mountains.